Supplemental Materials

GSA Data Repository 2018249

Joo et al., 2018, Anomalously low chemical weathering in fluvial sediment of a tropical watershed (Puerto Rico): Geology, https://doi.org/10.1130/G40315.1.

Figure DR1. Meters-thick soil and saprolite profile exposed within the RG drainage basin. Despite these thick soils and saprolite in the region, the fluvial sediments record significantly less chemical weathering, suggesting landslides are delivering less-weathered regolith to the stream system.

Methods

Sediment samples were collected in May 2014 from the Rio Guayanes (RG) stream system near Yabacoa in southeastern Puerto Rico (Tables DR1-2).

Table DR1. Characteristics of Rio Guayanés watershed (Southeastern Regional Climate Center, 2000).

Attributes	
Transect length	19.6 km
Drainage area	54.5 km^2
Relief	372 m
Mean annual temperature	26 ºC
Mean annual precipitation	2017 mm
Discharge	1.95 m^3/s

Each sediment sample was split using the cone-and-quartering method of Schumacher et al. (1991) to obtain a representative 100-250 g subsample, and then wet sieved to separate the gravel (>2 mm), sand (63 μm – 2 mm), and mud (<63 μm) fractions (Table DR3). Sand fractions of selected samples were further sieved to isolate medium sand (250 μm - 500 μm) for thin sections. The mud fraction was treated with buffered acetic acid (pH ~ 4.8) for 24 hours to remove carbonate, and with 30% hydrogen peroxide for 1 - 3 days to remove organic matter. After rinsing thoroughly, the mud fraction was freeze dried for x-ray diffraction (XRD) and geochemical analyses. Before freeze drying, approximately ~0.5 g of wet sample was collected for laser particle size analysis. Bedrock and saprolite samples were powdered with a McCrone micronizer (10 minutes/sample) prior to XRD and geochemical analysis. Table DR2 summarizes the analyses completed for each sediment sample.

Table DR2. List of sediment samples, their locations within the sampling transect, and types of analyses carried out for each sample.

Sample ID	Distance (km)	Granulometry	Medium sand thin section	XRD (mud)	Geochemistry (mud)
RG-a	0.0	✓	✓	✓	✓
RG-b	1.1	✓			
RG-c	2.3	✓			
RG-d	3.1	✓	✓		✓
RG-e	4.2	✓			
RG-f	6.6	✓	✓	✓	✓
RG-g	8.6	✓	✓	✓	✓
RG-h	11.5	✓			
RG-i	11.7	✓			
RG-j	12.2	✓			
RG-k	13.1	✓		✓	
RG-l	15.9	✓	✓	✓	✓
RG-m	19.6	✓			
RGTR-a	proximal tributary			✓	✓

Particle size distribution of the mud fraction was measured using a Beckman Coulter Laser Particle Size Analyzer LS230 (Table DR3). Prior to LPSA analysis, samples were treated with 2-3 drops of 0.5 % sodium hexametaphosphate to prevent flocculation, and sonicated for 1 minute. Bulk powder X-ray diffraction (XRD) analyses were conducted on samples of fresh and weathered bedrock and sediment (<63 μm fraction) using a Rigaku Ultima IV diffractometer. Bragg-Brentano geometry and Cu-K-alpha radiation (40 kV, 44 mA) were employed with a scintillation detector and data analysis was completed using Claysim software with the ICDD (International Center for Diffraction Data) PDF4+ database. Bulk chemical analyses of the bedrock and saprolite samples, and mud fractions of the sediment were conducted in a commercial lab (ALS-Chemex) using combined XRF and ICP-MS methods.

Thin sections were prepared for the bedrock samples, as well as the medium sand fraction collected from a subset of the sediment samples. Approximately 300 points were counted for each thin section using the Gazzi Dickinson method (Ingersoll et al., 1984). Thin sections for the bedrock samples were analyzed using a Cameca SX50 electron probe microanalyzer at the University of Oklahoma to determine chemical composition of plagioclase, potassium feldspar, and hornblende. At least five grains of each mineral species were selected for analysis and a minimum of five points were analyzed in each grain, typically in a transect from the center to the edge of the grain. The analyses performed for each sediment sample are summarized in Table DR1.

Results

Granulometry

Table DR3 Grainsize data from all sediment samples in this study.

		Wt % size fractions (sieving)			Volume % size fractions & grain size (LPSA)		
RG sediment	Distance (km)	Gravel	Sand	Mud	silt (bulk)	clay (bulk)	mode (μm)
RG-14-3 (a)	0	19.08	77.04	3.89	1.869	2.016	3.36
RG-14-4 (b)	1.1	18.26	78.44	3.29	2.328	0.965	19.76
RG-14-11 (c)	2.31	26.36	69.27	4.37	3.237	1.137	35.32
RG-14-A(4.5) (d)	3.05	36.12	59.34	4.54	3.404	1.135	45.75
RG-14-13 (e)	4.15	10.77	85.81	3.43	2.375	1.052	19.76
RG-14-5 (f)	6.61	0.94	91.72	7.35	5.893	1.455	50.22
RG-14-15 (g)	8.55	0.58	92.91	6.51	5.648	0.866	50.22
RG-14-7 (h)	11.51	0.95	92.95	6.1	4.117	1.982	37.97
RG-14-6 (i)	11.72	1.71	93.56	4.73	4.171	0.563	55.13
RG-14-8 (j)	12.24	6.82	85.36	7.82	6.398	1.424	45.75
RG-14-9 (k)	13.06	0	89	11	7.888	3.114	34.58
RG-14-10 (l)	15.89	6.12	92.94	0.94	0.738	0.203	45.75
RG-14-14 (m)	19.56	12.14	74.42	13.45	7.906	5.54	7.08

Bedrock mineralogy

Point counts and XRD analysis indicate that the granodiorite bedrock consists of plagioclase (~55%), quartz (~18%), K-feldspar (~12%), hornblende (~10%), chlorite (~7%), and accessory minerals (Table DR2). The quartz diorite bedrock is composed of plagioclase (~61%), quartz (~24%), and hornblende (~11%) with trace amounts of chlorite, K-feldspar, and accessory minerals (Table DR3). The metavolcanic bedrock is dominated by hornblende (~62%) and plagioclase (~32%) with accessory amounts of pyroxene and opaque minerals (~2%). Although the diorite bedrock does not crop out in the study area, the average modal composition of the diorite available from literature (Roberts et al, 1979; Table DR4) is similar to the quartz diorite, except for lower quartz (~4%) and higher hornblende (~25%) contents. The stochiometric composition of major minerals determined by electron microprobe in the bedrock appears in Table DR5. The average compositions of plagioclase (andesine; An_{40-49}) and hornblende from the granodiorite, quartz diorite, and metavolcanics are quite similar. The K-feldspar in the granodiorite corresponds to sanidine with <10% of Na-feldspar.

Table DR4. Mineralogy of bedrock determined by point counts and XRD analysis.

	Quartz	Plagioclase	K-feldspar	Hornblende	Mica	Chlorite	Acc.
Modal composition (vol. %)							
Granodiorite	20	57	11	10	0	5	0
Quartz diorite	26	60	0	11	0	1	2
Diorite	3.5	63	0	25	tr	tr	8
(Roberts et al., 1979)							
XRD analysis (wt. %)							
Granodiorite	17	53	13	9	<1	8	<1
Metavolcanics	0	36	<1	62	<1	<1	2
Quartz diorite	21	62	<1	11	8	2	2

Table DR5. Stoichiometries of major rock-forming minerals in the bedrock samples as determined by electron microprobe analysis.

Mineral in bedrock	Formula
Granodiorite	
Plagioclase	$Na_{0.59}Ca_{0.40}K_{0.01}Al_{1.39}Si_{2.60}O_8$
K-feldspar	$Na_{0.08}K_{0.89}Ba_{0.02}Al_{1.03}Si_{2.97}O_8$
Hornblende	$(Ca_{1.82}Na_{0.31}K_{0.13})(Mg_{2.80}Fe_{1.99}Al_{0.22})(Si_{7.02}Al_{0.98})O_{22}(OH)_2$
Quartz diorite	
Plagioclase	$Na_{0.48}Ca_{0.49}K_{0.01}Al_{1.50}Si_{2.50}O_8$
Hornblende	$(Ca_{1.84}Na_{0.12}K_{0.03})(Mg_{3.19}Fe_{1.72}Al_{0.14})(Si_7Al_{0.46})O_{22}(OH)_2$
Chlorite	$(Fe_{1.93}Mg_{2.66}Mn_{0.05})Al_{2.24}Si_{2.98}(OH)_8$
Metavolcanics	
Hornblende (phenocryst)	$(Ca_{1.85}Na_{0.60}K_{0.11})(Mg_{2.95}Fe_{1.59}Al_{0.57})(Si_{6.11}Al_{1.89})O_{22}(OH)_2$
Hornblende (matrix)	$(Ca_{1.90}Na_{0.15}K_{0.03})(Mg_{2.49}Fe_{2.33}Al_{0.30})(Si_{7.23}Al_{0.77})O_{22}(OH)_2$
Plagioclase (matrix)	$Na_{0.56}Ca_{0.43}K_{0.11}Al_{1.45}O_8$

Sediment mineralogy

The modal composition of the medium sand fraction from the main channel of the Rio Guayanés exhibits significantly higher quartz (~50%), lower plagioclase (~23%) and chlorite (<1%), and comparable K-feldspar and hornblende contents relative to the bedrock (Table DR6). Altered grains, which lack traces of primary minerals, are most abundant in the proximal sample (RG-a). Likewise, lithic fragments of the finer matrix of quartz diorite and metavolcanics is more abundant in the proximal samples. Except for the most distal analyzed sample (RG-l), relative proportions of quartz and K-feldspar become more abundant downstream, while plagioclase, altered grains, lithic fragments containing matrix material from the quartz diorite and metavolcanics, and hornblende decrease down transect. The medium sand fraction of the RG-l sample contains significantly more plagioclase and hornblende, and less quartz, but similar concentrations of biotite and lithic fragments than the more distal sand samples

Table DR6. Mineralogy (volume %) of medium sands as determined by point counts, and muds as determined by XRD analysis.

	Qtz	Pl	Ksp	Hb	Chl	Bt	Alt.	Matrix (QD)	Matrix (MV)	Kaol +Hal	Smec	Acc
Medium sand (250 – 500 µm)												
RG-a	43	20	8	7	1	4	10	6	1	-	-	4
RG-d	48	28	4	7	0	3	3	6	2	-	-	3
RG-f	54	21	8	5	0	4	5	2	1	-	-	4
RG-g	51	20	13	6	0	2	6	1	0	-	-	2
RG-l	44	26	11	10	1	1	4	2	0	-	-	1
Mud (<63 µm)												
RG-a	8	25	8	14	6	5	-	-	-	20	14	-
RG-f	8	19	9	19	5	7	-	-	-	34	-	-
RG-g	5	18	3	10	15	7	-	-	-	41	-	1
RG-k	4	17	3	9	15	7	-	-	-	45	-	1
RG-l	11	39	-	15	7	-	-	-	-	26	1	1
RG-sap	27	-	-	-	10	-	-	-	-	49	6	9

The mineralogy of the mud fraction contrasts with that of the medium sand fraction, exhibiting high contents of clay minerals (up to 45%; kaolinite, halloysite, and smectite), chlorite (~10 %), and hornblende (~13 %, Fig. 1D in main text; Table DR5). The proportions of minerals composing the mud fraction also change systematically from the proximal to more distal parts of the stream. For example, quartz, plagioclase, hornblende, and K-feldspar progressively decrease in the muds downstream, while kaolinite, halloysite and chlorite become enriched in the distal samples, except for the RG-l (Fig. 1D). The RG-l sample displays a much higher concentration

of quartz, plagioclase, and hornblende, and less kaolinite and halloysite than the other distal samples (Fig. 1D; Table DR5). Therefore, the concentration of primary minerals decreases, whereas the concentration of secondary minerals increases downstream, except for sample RG1 (Fig. 1E). The relative concentrations of primary and secondary minerals inverts as the stream enters the gorge, between RG-g and RG-l (Fig. 1E). Saprolite collected in the proximal part of the drainage basin is mostly composed of kaolinite and halloysite (~49 %), quartz (~27 %), chlorite (~10 %), and accessory oxides (~9 %).

Geochemistry

Concentrations of selected major oxides observed in bedrock, saprolite, and fine-grained sediment samples from the Rio Guayanés transect are plotted in Fig. DR2. CaO and Na_2O concentrations in the mud fraction are similar to those of the quartz diorite and granodiorite and generally decrease downstream (Fig.DR2A, B, Table DR6, also shown in Figure 1E,F in the main text). On the other hand, K_2O concentration progressively increases with distance along the transect (Fig. DR2C). Fe_2O_3 and MgO are enriched in the mud samples relative to the granodiorite and quartz diorite and decrease downstream (Fig. DR2D, E). The saprolite sample is depleted with respect to the bedrock samples for most of the cations shown in Fig. DR2, except for Fe_2O_3 and MgO; the saprolite Fe_2O_3 content is higher than the sediment and all three bedrock samples. MgO is present in the saprolite, but at lower concentrations than those observed in the bedrock samples.

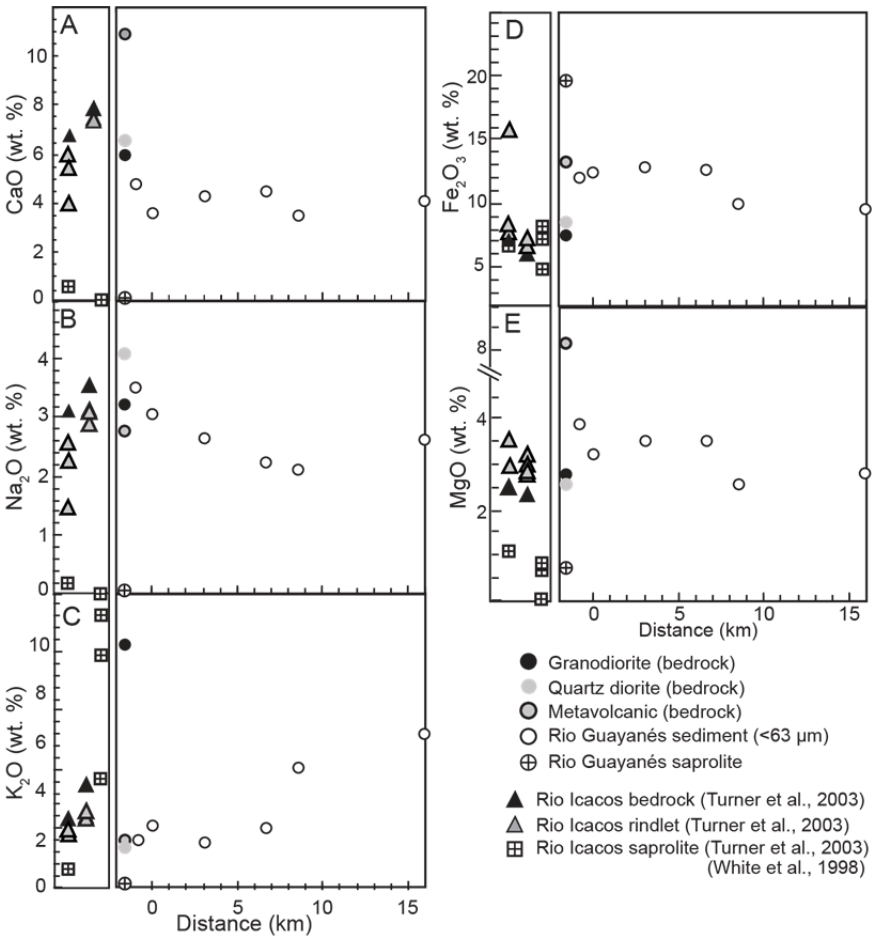

Figure DR2. Geochemical data observed in bedrock, saprolite, and mud fraction of RG fluvial sediment compared to other samples from Puerto Rico (A-E). Data from previous studies of weathering profiles developed in the Rio Icacos watershed in the Luquillo Experimental Forest, NE Puerto Rico are shown in the left pane of each plot (White et al., 1998; Turner et al., 2003).

Table DR7. Weight percent oxide bulk geochemistry

sample ID	source	SiO2	Al2O3	Fe2O3	CaO	MgO	Na2O	K2O	TiO2	MnO	P2O5
Luquillo Experimenta Forest (LEF) data											
SSa rock (0) -fresh	Turner et al. 2003	59.35	20.14	7.03	6.63	2.46	3.09	0.60	0.51	0.13	0.05
SSa 18.5 - rindlet	Turner et al. 2003	59.57	19.80	7.93	5.91	2.91	2.58	0.50	0.59	0.15	0.05
SSa 25 - rindlet	Turner et al. 2003	59.35	21.14	7.71	5.39	2.92	2.28	0.48	0.54	0.14	0.04
SSa 29.5 - most weathered rindlet	Turner et al. 2003	56.06	17.84	15.79	3.86	3.49	1.48	0.58	0.73	0.17	0.01
SSa sap (45) - saprolite	Turner et al. 2003	64.86	25.59	6.72	0.57	1.05	0.18	0.19	0.77	0.07	0.00
TC- fresh rock	Turner et al. 2003	59.13	19.44	6.15	7.82	2.32	3.54	0.90	0.47	0.12	0.11
TCa 2.5 - rindlet	Turner et al. 2003	60.20	17.85	7.16	7.29	2.87	3.12	0.67	0.54	0.16	0.15
TCa 15 - rindlet	Turner et al. 2003	59.63	18.38	7.12	7.34	3.00	3.12	0.62	0.51	0.16	0.11
TCa 25 - rindlet	Turner et al. 2003	60.54	17.18	7.35	7.33	3.23	2.90	0.66	0.55	0.17	0.09
TCa 40 - most weathered rindlet	Turner et al. 2003	60.23	18.41	6.71	7.42	2.78	3.12	0.61	0.49	0.14	0.09
Sap.b 0.76	White et al 1998	77.04	16.73	4.82	0.00	0.00	0.00	0.96	0.43	0.02	0.00
Sap.b 2.87	White et al 1998	65.00	24.42	7.31	0.00	0.70	0.00	2.00	0.51	0.05	0.00
Sap.b 7.13	White et al 1998	59.19	28.27	8.11	0.00	0.82	0.00	2.39	0.61	0.62	0.00

RG sediment	comment	distance (km)	SiO2	Al2O3	Fe2O3	CaO	MgO	Na2O	K2O	TiO2	MnO	P2O5
RG-14-SED-1 (RGTR-a)		-2	55.94	17.97	11.93	4.80	3.88	3.51	0.42	0.98	0.24	0.29
RG-14-SED-3 (RG-a)	RG-a	0	55.52	20.09	12.48	3.58	3.20	3.07	0.55	1.02	0.26	0.17
RG-14-SED-4.5 (A) (RG-d)	RG-d	3.1	54.85	19.97	12.84	4.26	3.55	2.66	0.41	1.01	0.23	0.16
RG-14-SED-5 (RG-f)	RG-f	6.6	55.32	19.55	12.73	4.49	3.49	2.24	0.52	1.17	0.27	0.16
RG-14-SED-10 (RG-l)	RG-l	15.9	57.04	21.22	9.50	4.13	2.75	2.62	1.33	0.82	0.31	0.18
RG-14-SED-15 (RG-g)	RG-g	8.6	56.78	22.52	10.06	3.52	2.59	2.11	1.03	0.90	0.25	0.16
RG-saprolite	saprolite	1	54.77	23.20	19.65	0.17	0.70	0.08	0.06	1.17	0.15	0.02
RB-14-BDRK-#2A	granodiorite	0	61.63	15.61	7.57	6.00	2.77	3.20	2.07	0.62	0.16	0.18
RG-14-BDRK-13	quartz diorite	0	61.24	15.66	8.53	6.53	2.52	4.09	0.35	0.68	0.21	0.11
RG-14-BDRK-13amp	metavolcanic	0	48.36	14.65	13.22	10.91	8.16	2.78	0.43	1.01	0.23	0.17

Weathering index comparisons and data

Table DR8. Weathering indices reported in Table 1 in the main text (after Price and Velbel, 2009)

Index	**Formula**	**Reference**
R	SiO_2/Al_2O_3	Ruxton (1968)
WIP	$100*(2Na_2O/0.35) + MgO/0.9 + 2K_2O/0.25 + CaO/0.7)$	Parker (1970)
V	$(Al_2O_3 + K_2O) / (MgO+CaO+Na_2O)$	Vogt (1927)
CIA	$100*[Al_2O_3 / (Al_2O_3+ CaO+Na_2O+K_2O)]$	Nesbitt and Young (1982)
CIW	$100*[Al_2O_3 / (Al_2O_3+ CaO+Na_2O)]$	Harnois (1988)
PIA	$100*[(Al_2O_3-K_2O) / (Al_2O_3+ CaO+Na_2O-K_2O)]$	Fedo et al. 1995
STI	$100*\{(SiO_2/TiO_2) / [(SiO_2/TiO_2) + (SiO_2/ Al_2O_3) + (Al_2O_3/TiO_2)]\}$	De Jayawardena and Izawa (1994)

Table DR9 . CIA data from the literature shown in figure 3B in the main text

Data source	soil	Country	region	Bedrock	MAT	MAP	SiO2	TiO2	Al2O3	Fe2O3	MgO	CaO	Na2O	K2O	CIA	molar Al2O3	molar CaO	molar Na2O	molar K2O
White et al 2001	Ultisol	USA	Georgia	granite (Panola granit	17	1240	82.43	1.94	8.94	2.78	0.21	0.14	0.45	3.10	67	0.088	0.003	0.007	0.033
White et al 2001	Ultisol	USA	Georgia	granite (Panola granit	17	1240	79.04	1.53	12.00	3.17	0.32	0.12	0.36	3.46	73	0.118	0.002	0.006	0.037
White et al 2001	Ultisol	USA	Georgia	granite (Panola granit	17	1240	67.48	1.46	20.98	6.15	0.53	0.12	0.33	2.96	84	0.206	0.002	0.005	0.031
White et al 2001	Ultisol	USA	Georgia	granite (Panola granit	17	1240	65.16	1.15	22.76	6.87	0.42	0.08	0.27	3.29	85	0.223	0.001	0.004	0.035
White et al 2001	Ultisol	USA	Georgia	granite (Panola granit	17	1240	64.46	1.30	23.35	7.27	0.47	0.06	0.25	2.83	87	0.229	0.001	0.004	0.030
White et al 2001	Ultisol	USA	Georgia	granite (Panola granit	17	1240	66.54	1.32	21.83	6.89	0.51	0.06	0.21	2.63	87	0.214	0.001	0.003	0.028
White et al 2001	Ultisol	USA	Georgia	granite (Panola granit	17	1240	64.11	1.23	23.71	7.39	0.51	0.06	0.21	2.77	87	0.233	0.001	0.003	0.029
White et al 2001	Ultisol	USA	Georgia	granite (Panola granit	17	1240	64.00	1.17	24.01	7.69	0.49	0.07	0.24	2.33	89	0.236	0.001	0.004	0.025
White et al 2001	Ultisol	USA	Georgia	granite (Panola granit	17	1240	64.54	1.26	23.27	7.51	0.41	0.05	0.17	2.79	87	0.228	0.001	0.003	0.030
White et al 2001	Ultisol	USA	Georgia	granite (Panola granit	17	1240	64.19	1.26	24.03	6.43	0.55	0.06	0.20	3.28	86	0.236	0.001	0.003	0.035
White et al 2001	Ultisol	USA	Georgia	granite (Panola granit	17	1240	64.72	1.35	22.85	6.80	0.77	0.06	0.14	3.31	85	0.224	0.001	0.002	0.035
White et al 2001	Ultisol	USA	Georgia	granite (Panola granit	17	1240	66.33	1.34	20.70	6.08	0.81	0.07	0.23	4.43	80	0.203	0.001	0.004	0.047
White et al 2001	Ultisol	USA	Georgia	granite (Panola granit	17	1240	69.36	1.48	16.60	6.22	1.17	0.06	0.21	4.90	74	0.163	0.001	0.003	0.052
White et al 2001	Ultisol	USA	Georgia	granite (Panola granit	17	1240	66.33	1.24	21.67	5.38	1.07	0.05	0.20	4.06	82	0.213	0.001	0.003	0.043
White et al 2001	Ultisol	USA	Georgia	granite (Panola granit	17	1240	67.19	1.30	20.15	5.81	1.00	0.05	0.22	4.27	80	0.198	0.001	0.004	0.045
White et al 2001	Ultisol	USA	Georgia	granite (Panola granit	17	1240	67.20	1.06	22.19	5.07	0.95	0.05	0.24	3.23	85	0.218	0.001	0.004	0.034
White et al 2001	Ultisol	USA	Georgia	granite (Panola granit	17	1240	68.55	1.29	19.43	5.48	0.94	0.07	0.21	4.03	80	0.191	0.001	0.003	0.043
White et al 2001	Ultisol	USA	Georgia	granite (Panola granit	17	1240	69.50	1.26	18.43	5.33	1.09	0.06	0.20	4.14	79	0.181	0.001	0.003	0.044
White et al 2001	Ultisol	USA	Georgia	granite (Panola granit	17	1240	65.65	1.16	20.16	5.34	1.19	0.09	0.51	5.91	73	0.198	0.002	0.008	0.063
Krull et al 2002	Ultisol	Kenya	Kakamega	Precambrian gneiss	20.4	1971	72.08	0.81	13.51	6.45	0.71	4.44	0.71	1.31	56	0.132	0.079	0.011	0.014
Krull et al 2002	Ultisol	Kenya	Kakamega	Precambrian gneiss	20.4	1971	74.77	0.90	14.97	7.04	0.30	0.20	0.30	1.51	86	0.147	0.004	0.005	0.016
Krull et al 2002	Ultisol	Kenya	Kakamega	Precambrian gneiss	20.4	1971	74.10	0.90	15.36	7.33	0.30	0.20	0.30	1.51	86	0.151	0.004	0.005	0.016
Krull et al 2002	Ultisol	Kenya	Kakamega	Precambrian gneiss	20.4	1971	72.79	1.00	16.37	7.63	0.30	0.20	0.30	1.41	87	0.161	0.004	0.005	0.015
Krull et al 2002	Ultisol	Kenya	Kakamega	Precambrian gneiss	20.4	1971	71.72	0.90	16.45	8.83	0.30	0.10	0.30	1.40	88	0.161	0.002	0.005	0.015
Krull et al 2002	Ultisol	Kenya	Kakamega	Precambrian gneiss	20.4	1971	72.07	1.00	16.92	7.91	0.30	0.10	0.30	1.40	89	0.166	0.002	0.005	0.015
Krull et al 2002	Ultisol	Kenya	Kakamega	Precambrian gneiss	20.4	1971	69.47	1.00	18.62	8.81	0.30	0.10	0.30	1.40	89	0.183	0.002	0.005	0.015
White et al 1998	Ultisol	PR	Rio Icacos	Quartz diorite	22	4200	77.03	0.43	16.73	4.82	0.01	0.01	0.01	0.96	94	0.164	0.000	0.000	0.010
White et al 1998	Ultisol	PR	Rio Icacos	Quartz diorite	22	4200	65.02	0.51	24.43	7.31	0.70	0.01	0.01	2.00	92	0.240	0.000	0.000	0.021
White et al 1998	Ultisol	PR	Rio Icacos	Quartz diorite	22	4200	75.45	0.77	9.32	10.34	1.05	0.01	0.01	3.05	74	0.091	0.000	0.000	0.032
Hieronymus et al. 2001	Ultisol	Cameroon	Dschang	granodiorite	20.4	1936	74.65	0.78	20.15	3.36	0.11	0.11	0.06	0.78	95	0.198	0.002	0.001	0.008
Hieronymus et al. 2001	Ultisol	Cameroon	Dschang	granodiorite	20.4	1936	59.83	2.15	26.29	9.97	0.06	0.11	0.11	1.47	93	0.258	0.002	0.002	0.016
Hieronymus et al. 2001	Ultisol	Cameroon	Dschang	granodiorite	20.4	1936	62.93	2.22	19.98	12.99	0.22	0.22	0.11	1.33	91	0.196	0.004	0.002	0.014
Hieronymus et al. 2001	Ultisol	Cameroon	Dschang	granodiorite	20.4	1936	56.51	2.03	23.22	12.99	1.28	0.32	0.11	3.53	84	0.228	0.006	0.002	0.037
Hieronymus et al. 2001	Ultisol	Cameroon	Dschang	granodiorite	20.4	1936	57.85	2.06	22.14	10.45	2.93	0.22	0.22	4.12	81	0.217	0.004	0.004	0.044
Hamdan and Burnham 1996	Oxisol	Malaysia	Pahang	granite	26.5	2871	75.82	0.16	20.56	2.29	0.13	0.02	0.02	1.00	95	0.202	0.000	0.000	0.011
Hamdan and Burnham 1996	Oxisol	Malaysia	Pahang	granite	26.5	2871	66.10	0.21	26.51	5.16	0.30	0.01	0.02	1.70	93	0.260	0.000	0.000	0.018
Cooler climate																			
Ohlander et al 2000	Spodosol	Sweden	Kalix	granite till	1	509	69.26	1.56	12.99	6.38	0.81	2.38	3.76	2.87	49	0.127	0.042	0.061	0.030
Ohlander et al 2000	Spodosol	Sweden	Kalix	granite till	1	509	60.47	1.22	16.44	9.23	2.64	4.20	3.62	2.17	51	0.161	0.075	0.058	0.023
Ohlander et al 2000	Spodosol	Sweden	Kalix	granite till	1	509	61.83	1.38	14.39	8.46	2.95	4.79	3.87	2.35	45	0.141	0.085	0.062	0.025
Ohlander et al 2000	Spodosol	Sweden	Kalix	granite till	1	509	72.91	1.00	13.36	2.46	0.75	2.52	3.52	3.48	49	0.131	0.045	0.057	0.037
Ohlander et al 2000	Spodosol	Sweden	Kalix	granite till	1	509	65.31	0.80	17.29	6.10	1.46	2.96	3.40	2.68	55	0.170	0.053	0.055	0.028
Ohlander et al 2000	Spodosol	Sweden	Kalix	granite till	1	509	67.87	0.86	14.06	5.05	1.69	3.54	3.85	3.08	47	0.138	0.063	0.062	0.033
McAlister and Smith 1997	spodosol	Ireland	Mourne Mts	Granite	8.5	1019	78.28	0.41	12.45	2.13	0.92	0.37	1.99	3.46	62	0.122	0.007	0.032	0.037
McAlister and Smith 1997	spodosol	Ireland	Mourne Mts	Granite	8.5	1019	78.34	0.16	12.60	1.55	0.31	0.16	2.22	4.65	58	0.124	0.003	0.036	0.049
McAlister and Smith 1997	spodosol	Ireland	Mourne Mts	Granite	8.5	1019	60.58	0.27	31.68	2.29	0.51	0.08	1.25	3.35	84	0.311	0.001	0.020	0.036
McAlister and Smith 1997	spodosol	Ireland	Mourne Mts	Granite	8.5	1019	79.51	0.28	11.91	1.29	0.15	0.01	1.53	5.31	59	0.117	0.000	0.025	0.056
Lee et al, 2004	Gelisol	West Antarct	South Shetlar	granodiorite	-1.8	437.6	62.89	0.76	18.30	7.85	3.03	2.40	2.53	2.23	63	0.180	0.043	0.041	0.024
Lee et al, 2004	Gelisol	West Antarct	South Shetlar	granodiorite	-1.8	437.6	57.85	0.86	19.49	8.25	3.57	4.99	3.56	1.44	54	0.191	0.089	0.057	0.015
Lee et al, 2004	Gelisol	West Antarct	South Shetlar	granodiorite	-1.8	437.6	64.66	0.74	18.43	5.98	2.40	2.29	2.70	2.80	61	0.181	0.041	0.044	0.030
Lee et al, 2004	Gelisol	West Antarct	South Shetlar	granodiorite	-1.8	437.6	67.11	0.56	15.98	4.60	1.76	3.16	3.77	3.07	51	0.157	0.056	0.061	0.033
Lee et al, 2004	Gelisol	West Antarct	South Shetlar	granodiorite	-1.8	437.6	60.98	0.96	16.96	10.19	1.84	3.65	3.51	1.91	54	0.166	0.065	0.057	0.020

Modern estuarine sediment

See Li and Yang (2010) for the compilation of modern estuarine sediment

Table DR10. Data sources for CIA values within figure 3C in the main text.

Material listed in Fig 3C	Source	age	comments
Bighorn Basin	Adams et al 2011	PETM	
Spain coal bearing	Goldberg and Humayun 2010	Permian	
Baltic paleosol	Liivamagi 2014	Neoproterozoic	
China river suspended particulate matter	Shao & Yang 2012	modern	Zhujiang (river)
China river bank and floodplain	Shao & Yang 2012	modern	Zhujiang (river)
Taiwan river	Shao & Yang 2012	modern	Lanyang & Heping
Pearl river delta	Wan et al 2015	modern	bulk sediment
Rio Icacos saprolite	White et al 1998		
Rio Icacos saprolite	Turner et al 2003		
Rio Icacos Rindlet	Turner et al 2003		
Rio Icacos soil	White et al 1998		
Georgia Panola granite soil	White et al 2001		
Georgia panola granite saprolite	White et al 2001		
Weathered panola granite	White et al 2001		
Cameroon soil	Hieronymus et al 2001		
Malaysia soil and sap	Hamdan and Burnham 1996	soil	
Kenya soil	Krull et al 2002	soil	

References

Adams, J. S., Kraus, M. J., & Wing, S. L. (2011). Evaluating the use of weathering indices for determining mean annual precipitation in the ancient stratigraphic record. *Palaeogeography, Palaeoclimatology, Palaeoecology*, *309*(3), 358-366.

De Jayawardena and Izawa (1994) A new chemical index of weathering for metamorphic silicate rocks in tropical regions: A study from Sri Lanka. Engineering geology, C. 36, 303-310.

De Vos, W., Tarvainen, T., Salminen, R., Reeder, S., De Vivo, B., Demetriades, A., ... & O'Connor, P. J. (2006). Geochemical atlas of Europe. Part 2. *Interpretation of geochemical maps, additional tables, figures, maps and related publications. Geological Survey of Finland, Espoo*.

Drever, J. I. (1988). *The geochemistry of natural waters* (Vol. 437). Englewood Cliffs: prentice Hall.

Fedo, C. M., Wayne Nesbitt, H., & Young, G. M. (1995). Unraveling the effects of potassium metasomatism in sedimentary rocks and paleosols, with implications for paleoweathering conditions and provenance. *Geology*, *23*(10), 921-924.

Gao, S., Rudnick, R. L., Yuan, H. L., Liu, X. M., Liu, Y. S., Xu, W. L., ... & Wang, Q. H. (2004). Recycling lower continental crust in the North China craton. *Nature*, *432*(7019), 892-897.

Harnois, L. (1988). The CIW index: a new chemical index of weathering. *Sedimentary geology*, *55*(3-4), 319-322.

Goldberg, K., & Humayun, M. (2010). The applicability of the Chemical Index of Alteration as a paleoclimatic indicator: An example from the Permian of the Paraná Basin, Brazil. *Palaeogeography, Palaeoclimatology, Palaeoecology*, *293*(1), 175-183.

Hamdan, J., & Bumham, C. P. (1996). The contribution of nutrients from parent material in three deeply weathered soils of Peninsular Malaysia. *Geoderma*, *74*(3-4), 219-233.

Ingersoll, R. V., Bullard, T. F., Ford, R. L., Grimm, J. P., Pickle, J. D., & Sares, S. W. (1984). The effect of grain size on detrital modes: a test of the Gazzi-Dickinson point-counting method. *Journal of Sedimentary Research*, *54*(1), 103-116.

Kretzschmar, R., Robarge, W. P., & Amoozegar, A. (1994). Filter efficiency of three saprolites for natural clay and iron oxide colloids. *Environmental science & technology*, *28*(11), 1907-1915.

Krull, E. S., Bestland, E. A., & Gates, W. P. (2002). Soil organic matter decomposition and turnover in a tropical ultisol: evidence from δ13C, δ15N and geochemistry. *Radiocarbon*, *44*(1), 93-112.

Lee, Y. I., Lim, H. S., & Yoon, H. I. (2004). Geochemistry of soils of King George Island, South Shetland Islands, West Antarctica: implications for pedogenesis in cold polar regions. *Geochimica et Cosmochimica Acta*, *68*(21), 4319-4333.

Li, C., & Yang, S. (2010). Is chemical index of alteration (CIA) a reliable proxy for chemical weathering in global drainage basins?, *American Journal of Science*, *310*(2), 111-127.

Liivamägi, S., Somelar, P., Mahaney, W. C., Kirs, J., Vircava, I., & Kirsimäe, K. (2014). Late Neoproterozoic Baltic paleosol: Intense weathering at high latitude?. *Geology*, *42*(4), 323-326.

McAlister, J. J., & Smith, B. J. (1997). Geochemical trends in Early Tertiary palaeosols from northeast Ireland: a statistical approach to assess element behaviour during weathering. *Geological Society, London, Special Publications*, *120*(1), 57-65.

McBride, M. B. (1994). Environmental chemistry of soils. *Environmental chemistry of soils.*

Nesbitt, H., & Young, G. M. (1982). Early Proterozoic climates and plate motions inferred from major element chemistry of lutites. *Nature*, *299*(5885), 715.

Ohta, T., & Arai, H. (2007). Statistical empirical index of chemical weathering in igneous rocks: A new tool for evaluating the degree of weathering. *Chemical Geology*, *240*(3), 280-297.

Parker, A. (1970). An index of weathering for silicate rocks. *Geological Magazine*, *107*(6), 501-504.

Roberts, C. L., Cram, C. M., Pease Jr, M. H., & Tischler, M. S. (1979). *Geologic map of the Yabucoa and Punta Tuna quadrangles, Puerto Rico* (No. 1086).

Ruxton, B. P. (1968). Measures of the degree of chemical weathering of rocks. *The Journal of Geology*, *76*(5), 518-527.

Shao, J., & Yang, S. (2012). Does chemical index of alteration (CIA) reflect silicate weathering and monsoonal climate in the Changjiang River basin?. *Chinese science bulletin*, *57*(10), 1178-1187.

Southeastern Regional Climate Center http://www.sercc.com

Turner, B. F., Stallard, R. F., & Brantley, S. L. (2003). Investigation of in situ weathering of quartz diorite bedrock in the Rio Icacos basin, Luquillo Experimental Forest, Puerto Rico. *Chemical Geology*, *202*(3), 313-341.

Vogt, T. (1927) Sulitjelmafeltets geologiogpetrografi. Nor. Geol. Unders. 121: 1-560

Wan, S., Toucanne, S., Clift, P. D., Zhao, D., Bayon, G., Yu, Z., ... & Li, A. (2015). Human impact overwhelms long-term climate control of weathering and erosion in southwest China. *Geology*, *43*(5), 439-442.

White, A. F., Blum, A. E., Schulz, M. S., Vivit, D. V., Stonestrom, D. A., Larsen, M., ... & Eberl, D. (1998). Chemical weathering in a tropical watershed, Luquillo Mountains, Puerto Rico: I. Long-term versus short-term weathering fluxes. *Geochimica et Cosmochimica Acta*, *62*(2), 209-226.

White, A. F., Bullen, T. D., Schulz, M. S., Blum, A. E., Huntington, T. G., & Peters, N. E. (2001). Differential rates of feldspar weathering in granitic regoliths. *Geochimica et Cosmochimica Acta*, *65*(6), 847-869.